Crucial lncRNAs associated with adipocyte differentiation from human adipose-derived stem cells based on co-expression and ceRNA network analyses

Kana Chen[1], Shujie Xie[2] and Wujun Jin[1]

[1] Department of Plastic Surgery, Hwa Mei Hospital, University of Chinese Academy of Sciences, Ningbo, Zhejiang, China
[2] Department of Hepatobiliary Surgery, Hwa Mei Hospital, University of Chinese Academy of Sciences, Ningbo, Zhejiang, China

ABSTRACT

Background: Injection of adipose-derived stem cells (ASCs) is a promising treatment for facial contour deformities. However, its treatment mechanisms remain largely unknown. The study aimed to explain the molecular mechanisms of adipogenic differentiation from ASCs based on the roles of long noncoding RNAs (lncRNAs).

Methods: Datasets of mRNA–lncRNA (GSE113253) and miRNA (GSE72429) expression profiling were collected from Gene Expression Omnibus database. The differentially expressed genes (DEGs), lncRNAs (DELs) and miRNAs (DEMs) between undifferentiated and adipocyte differentiated human ASCs were identified using the Linear Models for Microarray Data method. DELs related co-expression and competing endogenous RNA (ceRNA) networks were constructed. Protein–protein interaction (PPI) analysis was performed to screen crucial target genes.

Results: A total of 748 DEGs, 17 DELs and 51 DEMs were identified. A total of 13 DELs and 279 DEGs with Pearson correlation coefficients > 0.9 and p-value < 0.01 were selected to construct the co-expression network. A total of 151 interaction pairs among 112 nodes (10 DEMs; eight DELs; 94 DEGs) were obtained to construct the ceRNA network. By comparing the lncRNAs and mRNAs in two networks, five lncRNAs (SNHG9, LINC02202, UBAC2-AS1, PTCSC3 and myocardial infarction associated transcript (MIAT)) and 32 genes (i.e., such as phosphoinositide-3-kinase regulatory subunit 1 (PIK3R1), protein tyrosine phosphatase receptor type B (PTPRB)) were found to be shared. PPI analysis demonstrated PIK3R1 , forkhead box O1 (FOXO1; a transcription factor) and estrogen receptor 1 (ESR1) were hub genes, which could be regulated by the miRNAs that interacted with the above five lncRNAs, such as LINC02202-miR-136-5p-PIK3R1, LINC02202-miR-381-3p-FOXO1 and MIAT-miR-18a-5p-ESR1. LINC02202 also could directly co-express with PIK3R1. Furthermore, PTPRB was predicted to be modulated by co-expression with LINC01119.

Conclusion: MIAT, LINC02202 and LINC01119 may be potentially important, new lncRNAs associated with adipogenic differentiation of ASCs. They may be involved in adipogenesis by acting as a ceRNA or co-expressing with their targets.

Submitted 15 May 2019
Accepted 24 July 2019
Published 6 September 2019

Corresponding author
Wujun Jin, wujunjin2019@163.com

Academic editor
Kenta Nakai

Additional Information and Declarations can be found on page 15

DOI **10.7717/peerj.7544**

Subjects Bioinformatics, Computational Biology, Genomics, Surgery and Surgical Specialties
Keywords Human adipose tissue-derived stromal stem cells, Adipogenic differentiation, ceRNA, lncRNA, miRNA, Co-expression

INTRODUCTION

Autologous adipose tissue grafting has been a widely accepted surgical tool for anti-aging cosmetics (*Charles-De-Sá et al., 2015*) and reconstructive restoration of various congenital or acquired facial soft tissue deformities (*Bashir et al., 2018*). However, conventional fat grafting procedure needs to be repeated multiple times to achieve satisfactory results (*Bashir et al., 2018*), which may be associated with the low graft survival rate and poor revascularization (*Ma et al., 2015*). To overcome these two limitations, recent scholars propose to combine with additional autologous adipose-derived stem cells (ASCs) which have the ability to differentiate into mature adipocytes to supplement apoptotic cells and secrete angiogenic growth factors to enhance angiogenesis (*Bashir et al., 2018*; *Kotaro et al., 2008*; *Philips, Marra & Rubin, 2014*). The clinical trials also confirm that supplementation of ASCs to adipose grafts is superior to conventional lipoinjection for facial recontouring (*Bashir et al., 2018*; *Kotaro et al., 2008*). Nevertheless, the use of autologous ASCs has not been FDA-approved. This may be because there still remains a huge gap in understanding the potential mechanisms of ASCs for adipocyte differentiation.

Increasing evidence has suggested long noncoding RNAs (lncRNAs), a class of noncoding RNAs more than 200 nucleotides, play crucial roles in adipogenesis for ASCs. For example, *Nuermaimaiti et al. (2018)* demonstrated that knockdown of HOXA11-AS1 inhibited adipocyte differentiation, leading to suppression of adipogenic-related gene transcription, as well as decreased lipid accumulation in ASCs. *Huang et al. (2017)* observed knockdown of MIR31HG inhibited adipocyte differentiation, whereas overexpression of MIR31HG promoted adipogenesis in vitro and in vivo. MEG3 was also found to be downregulated during adipogenesis of ASCs. Functional analysis showed that knockdown of MEG3 promoted adipogenic differentiation of ASCs (*Li et al., 2017*). Furthermore, current research shows lncRNAs, on one hand, functions as microRNA (miRNAs) sponges to bind the miRNA response elements and regulate miRNA-mediated gene silencing (i.e., competing endogenous RNA (ceRNA) hypothesis); and, on the other hand, directly influences their neighboring genes expression by chromatin remodeling or transcriptional control (co-expression model) (*Huang et al., 2016*; *Li, Ao & Wu, 2017*). These theories have also been reported in ASCs. *Li, Ao & Wu (2017)* proved downregulated MEG3 may be insufficient to sponge miR-140-5p and lead to its upregulation during adipogenesis in ASCs. *Huang et al. (2017)* revealed inhibition of MIR31HG reduced the enrichment of active histone markers, histone H3 lysine 4 trimethylation and acetylation in the promoter of fatty acid binding protein 4, resulting in suppression of its expression and adipogenesis. However, the adipogenic differentiation related lncRNAs and its mechanisms of ASCs remains rarely reported.

The present study aimed to identify crucial lncRNAs involved in adipocyte differentiation of ASCs by constructing lncRNA–miRNA–mRNA ceRNA network and lncRNA–mRNA co-expression network using high throughput analysis data. Our findings

might offer greater insights into the molecular mechanisms of adipocyte differentiation from ASCs and provide potentially new targets for inducing adipogenesis.

MATERIALS AND METHODS

Collection of microarray data

GSE113253 (*Rauch et al., 2019*) and GSE72429 datasets (Supplemental Information 1) were downloaded from the Gene Expression Omnibus (GEO) database (http://www.ncbi.nlm.nih.gov/geo/). GSE113253 dataset applied the high throughput sequencing methodology to simultaneously detect the lncRNA and mRNA expression profiles in two repeats of undifferentiated human ASCs and 10 repeats of adipogenic differentiation cells using an Illumina HiSeq 1500 instrument, which was submitted to GEO on April 17, 2018. GSE72429 dataset analyzed the miRNA expression profile in four undifferentiated human ASCs and two adipogenic differentiation cells using an Agilent-031181 Unrestricted_Human_miRNA_V16.0_Microarray (miRBase release 16.0 miRNA ID version), which was submitted to GEO on August 27, 2015.

Differential expression analysis

The normalized series matrix files of each dataset were downloaded from GEO. Following re-annotation according to corresponding platform (GPL18460), the expression values of the lncRNAs and mRNAs in GSE113253 were obtained. The differentially expressed genes (DEGs), lncRNAs (DELs) and miRNAs (DEMs) were identified using the Linear Models for Microarray Data method software (version 3.34.0; *Ritchie et al., 2015*). p-Value was adjusted by using Benjamini–Hochberg method to avoid false positives. The heatmap was constructed to present the expression difference of DEGs, DELs and DEMs in different samples using the pheatmap package (version: 1.0.8; *Kolde, 2019*) based on Euclidean distance.

Co-expression network between lncRNA and mRNA

The co-expression network was constructed based on the correlation analysis between DELs and DEGs. Pearson correlation coefficients were calculated using the Weighted Gene Correlation Network Analysis (*Langfelder & Horvath, 2016*) algorithm to assess the correlation. Only the co-expressed pairs with absolute value of Pearson correlation coefficients ≥ 0.9 and $p < 0.01$ were selected to draw the network using Cytoscape (version 3.4; *Shannon et al., 2001–2008*; *Kohl, Wiese & Warscheid, 2011*).

CeRNA regulatory network among DELs, DEMs and DEGs

The DEMs related target genes were predicted using the miRwalk database (version 2.0; *Dweep & Gretz, 2015a*, *2015b*) which provides 12 prediction algorithms (miRWalk, MicroT4, miRanda, miRBridge, miRDB, miRMap, miRNAMap, PICTAR2, PITA, RNA22, RNAhybrid, Targetscan). Only the miRNA-target gene interaction pairs that were predicted in at least eight databases were used. The target genes were then overlapped with the DEGs to screen negatively correlated DEM–DEG interaction pairs. The miRcode (http://www.mircode.org/) (*Jeggari, Marks & Larsson, 2012*), starBase (version 2.0; *Yang, 2010–2013*;

Li et al., 2014) and DIANA-LncBase (version 2.0; *Paraskevopoulou et al., 2019*; *Paraskevopoulou et al., 2013*) databases were used to predict the interaction relationship between DELs and DEMs. The negatively correlated DEL–DEM interaction pairs were left for further analysis. The DEL–DEM and DEM–DEG interactors were integrated to construct the ceRNA network, which was visualized using Cytoscape.

Protein–protein interaction network

Protein–protein interaction (PPI) data of DEGs in the ceRNA network was collected from Search Tool for the Retrieval of Interacting Genes (STRING; version 10.0; *Szklarczyk et al., 2019*) database (*Szklarczyk et al., 2015*). Only interactions with combined score >0.4 were selected to construct the PPI network. Several topological features of the nodes (protein) in the PPI network were calculated using the CytoNCA plugin in cytoscape software (*Tang, Li & Wang, 2014*; *Tang et al., 2015*) to screen hub genes, including degree, eigenvector, betweenness and closeness centrality. Furthermore, transcription factors were predicted using iRegulon (*Janky et al., 2014*) in Cytoscape and then integrated to the PPI network.

Function enrichment analysis

Gene ontology (GO) and Kyoto Encyclopedia of Genes and Genomes (KEGG) pathway enrichment analyses were performed using the Database for Annotation, Visualization and Integrated Discovery online tool (version 6.8; http://david.abcc.ncifcrf.gov) (*Huang, Sherman & Lempicki, 2009*) to reveal the function of DEGs. $p < 0.05$ was set as the cut-off value.

RESULTS

Differential expression analysis

Due to the fact that fewer DEGs, DELs and DEMs were identified if adjusted *p*-value was defined as the statistical threshold; therefore, genes, lncRNAs and miRNAs were believed to be differentially expressed in this study when their |log2fold change (FC)| was more than 1 and *p*-value was less than 0.05. Based on these given thresholds, a total of 748 protein-coding genes (360, upregulated; 388, downregulated) (Table 1; Supplemental Information 2) and 17 lncRNAs (nine upregulated; eight downregulated) (Table 1; Supplemental Information 2) were found to be differentially expressed in adipogenic differentiation cells compared with undifferentiated cells in GSE113253 dataset. Among them, 121 DEGs (such as forkhead box O1 (FOXO1), protein tyrosine phosphatase receptor type B (PTPRB)) and two DELs (SH3RF3-AS1, LINC01119) had adjusted *p*-value < 0.05, indicating they were especially crucial for adipogenic differentiation. A total of 51 miRNAs (Table 1; Supplemental Information 2) were identified to be significantly differentially expressed in GSE72429 within the $p < 0.05$ and $|\log2FC| > 1$ criteria. Among them, 20 DEMs (particularly, miR-663 and miR-3607-3p, with adjusted *p*-value < 0.05) were upregulated and 31 DEMs (particularly, miR-150*, miR-4271, miR-371-5p and miR-134, with adjusted *p*-value < 0.05) were downregulated. Additionally, hierarchical clustering of DEGs (Fig. 1A),

Table 1 Differentially expressed genes, lncRNAs and miRNAs.

	logFC	*p*-Value		logFC	*p*-Value		logFC	*p*-Value
CRLF1	5.31	1.55*E*-10*	SH3RF3-AS1	4.00	8.45*E*-06*	miR-663	6.22	2.53*E*-06*
ZBTB16	6.71	2.90*E*-10*	LINC01554	2.06	1.19*E*-02	miR-3607-3p	5.55	3.91*E*-06*
COMP	6.30	5.07*E*-10*	SNHG9	2.04	1.45*E*-02	miR-455-3p	2.93	2.91*E*-04
FOXO1	4.98	3.85*E*-09*	LINC01914	2.35	1.74*E*-02	miR-455-5p	5.68	6.45*E*-03
LMO3	4.92	5.15*E*-09*	C18orf65	1.61	2.40*E*-02	miR-30c	1.45	7.52*E*-03
KLF15	5.19	6.31*E*-09*	LINC02202	1.65	4.06*E*-02	miR-181b	1.45	1.26*E*-02
MT1G	4.71	1.68*E*-08*	UBAC2-AS1	1.69	4.17*E*-02	miR-92a	1.33	1.33*E*-02
NEFL	5.50	3.12*E*-08*	LOH12CR2	1.86	4.55*E*-02	miR-609	2.43	2.97*E*-02
NRCAM	4.84	5.19*E*-08*	OSER1-DT	1.92	4.99*E*-02	miR-339-3p	2.48	2.99*E*-02
PCSK1	4.32	1.05*E*-07*	LINC01119	−3.77	1.80*E*-04*	miR-887	2.65	3.07*E*-02
FRAS1	6.29	1.14*E*-07*	SERPINB9P1	−2.35	4.55*E*-03	miR-124	2.70	3.10*E*-02
PDK4	5.95	1.50*E*-07*	MIAT	−3.24	5.06*E*-03	miR-3653	1.01	3.17*E*-02
PER1	3.90	3.26*E*-07*	LINC00601	−1.85	1.98*E*-02	miR-652	2.90	3.20*E*-02
IL18R1	4.60	4.67*E*-07*	LINC00211	−1.48	3.31*E*-02	miR-769-5p	2.91	3.21*E*-02
MT1X	3.60	4.76*E*-07*	PTCSC3	−1.72	3.81*E*-02	miR-18a	3.08	3.30*E*-02
MT1M	3.82	4.86*E*-07*	CYTOR	−1.49	4.63*E*-02	miR-1290	3.31	3.42*E*-02
PDE4D	4.06	1.03*E*-06*	LINC00865	−1.53	4.85*E*-02	miR-1973	1.15	3.45*E*-02
SERPINA3	4.91	1.61*E*-06*	SH3RF3-AS1	4.00	8.45*E*-06*	miR-30a*	1.84	3.87*E*-02
RASD1	4.46	1.68*E*-06*				miR-132	1.23	3.87*E*-02
IL1RL1	5.91	1.71*E*-06*				miR-K12-5*	2.93	4.46*E*-02
GALNT15	4.46	2.24*E*-06*				miR-150*	−6.28	3.37*E*-07*
FKBP5	3.42	2.37*E*-06*				miR-4271	−6.29	1.43*E*-06*
ELOVL3	3.94	2.95*E*-06*				miR-371-5p	−6.51	1.79*E*-06*
HSD11B1	3.63	3.39*E*-06*				miR-134	−6.39	3.26*E*-06*
PIK3R1	2.42	5.88*E*-04				miR-146b-5p	−5.32	4.43*E*-04
ARNT2	−5.34	3.01*E*-08*				miR-136	−2.12	1.12*E*-03
FGF9	−4.24	2.78*E*-07*				miR-199b-5p	−2.81	4.17*E*-03
IL6	−5.82	2.90*E*-07*				miR-29b	−1.80	5.88*E*-03
OXTR	−5.64	2.06*E*-06*				miR-376b	−4.36	9.46*E*-03
RTKN2	−4.16	2.83*E*-06*				miR-130b	−1.33	1.20*E*-02
PTPRB	−4.63	4.43*E*-06*				miR-218	−3.94	1.22*E*-02
SHROOM3	−3.37	7.27*E*-06*				miR-154*	−4.42	1.25*E*-02
RGS4	−3.28	8.10*E*-06*				miR-381	−1.11	1.31*E*-02
ARHGEF28	−3.39	1.08*E*-05*				miR-377	−1.23	1.45*E*-02
GPR68	−3.67	1.46*E*-05*				miR-503	−1.85	1.59*E*-02
VCAM1	−4.30	1.59*E*-05*				miR-337-5p	−1.04	2.13*E*-02
ATP8B1	−3.51	1.80*E*-05*				miR-3132	−1.24	2.18*E*-02
CNIH3	−3.42	2.61*E*-05*				miR-362-3p	−3.63	2.18*E*-02
ZSWIM4	−3.17	2.67*E*-05*				miR-3659	−1.28	2.23*E*-02
EPHA2	−3.36	3.35*E*-05*				miR-H6	−1.49	2.31*E*-02
CDCP1	−4.48	3.93*E*-05*				miR-135a*	−2.56	2.37*E*-02

(Continued)

Table 1 (continued).

	logFC	*p*-Value	logFC	*p*-Value		logFC	*p*-Value
FRMD5	−3.14	4.35*E*-05*			miR-29b-1*	−1.79	2.61*E*-02
NR3C2	−2.88	4.40*E*-05*			miR-376c	−1.09	2.64*E*-02
GREM2	−3.48	4.91*E*-05*			miR-193a-3p	−1.35	2.79*E*-02
CEMIP	−4.84	4.92*E*-05*			miR-140-3p	−1.07	2.84*E*-02
BIRC3	−3.21	8.05*E*-05*			miR-642b	−3.77	3.04*E*-02
RBM24	−3.28	9.30*E*-05*			miR-125a-3p	−1.20	3.16*E*-02
KY	−3.20	1.08*E*-04*			miR-140-5p	−1.26	3.51*E*-02
NUAK2	−2.93	1.21*E*-04*			miR-718	−2.64	4.41*E*-02
FGF1	−4.52	1.27*E*-04*			miR-299-3p	−4.10	4.83*E*-02
ESR1	−1.911	1.48*E*-02			miR-376a*	−4.02	4.99*E*-02

Note:
All the differentially expressed miRNAs and lncRNAs were shown, but only top 25 upregulated and downregulated mRNAs as well as crucial genes were displayed.
FC, fold change.
p-Value with asterisk indicated their adjusted *p*-value were also less than 0.05.

DELs (Fig. 1B) and DEMs (Fig. 1C) expression levels indicated the differentiated samples could be well distinguished from the undifferentiated samples.

Construction of co-expression and ceRNA networks

A total of 13 DELs and 279 DEGs with Pearson correlation coefficients > 0.9 and *p*-value < 0.01 were selected to construct the lncRNA–mRNA co-expression network, which contained 440 positive connections (Fig. 2; Supplemental Information 3).

Based on at least eight database analyses in miRwalk 2.0 and negatively correlated principles, a total of 79 downregulated DEGs were predicted to be regulated by eight upregulated DEMs, while 128 upregulated DEGs were predicted to be regulated by 32 downregulated DEMs. Using the starBase database, 355 miRNAs were predicted to interact with 25 DELs; using the miRcode database, 192 miRNAs were predicted to interact with eight DELs; using the DIANA-LncBase database, 1,343 miRNAs were predicted to interact with 15 DELs. After overlapping the DEMs that interacted with DELs and DEMs that regulated DEGs, 151 interaction pairs among 112 nodes (10 DEMs, four upregulated and six downregulated; eight DELs, four upregulated and four downregulated; 94 DEGs, 46 upregulated and 48 downregulated) were obtained, which were used for constructing the ceRNA network (Fig. 3; Supplemental Information 4).

PPI network

Protein–protein interaction pairs were predicted for the 94 DEGs in the ceRNA network using the STRING database, which resulted in 80 interaction relationship pairs that were screened between 58 nodes (24 upregulated and 34 downregulated) (Fig. 4). Phosphoinositide-3-kinase regulatory subunit 1 (PIK3R1), FYN proto-oncogene, Src family tyrosine kinase and estrogen receptor 1 (ESR1) were considered as hub genes in the PPI network because they ranked the top 10 in all four topological features (Table 2). In addition, FOXO1, which was included in the PPI network, was predicted as a

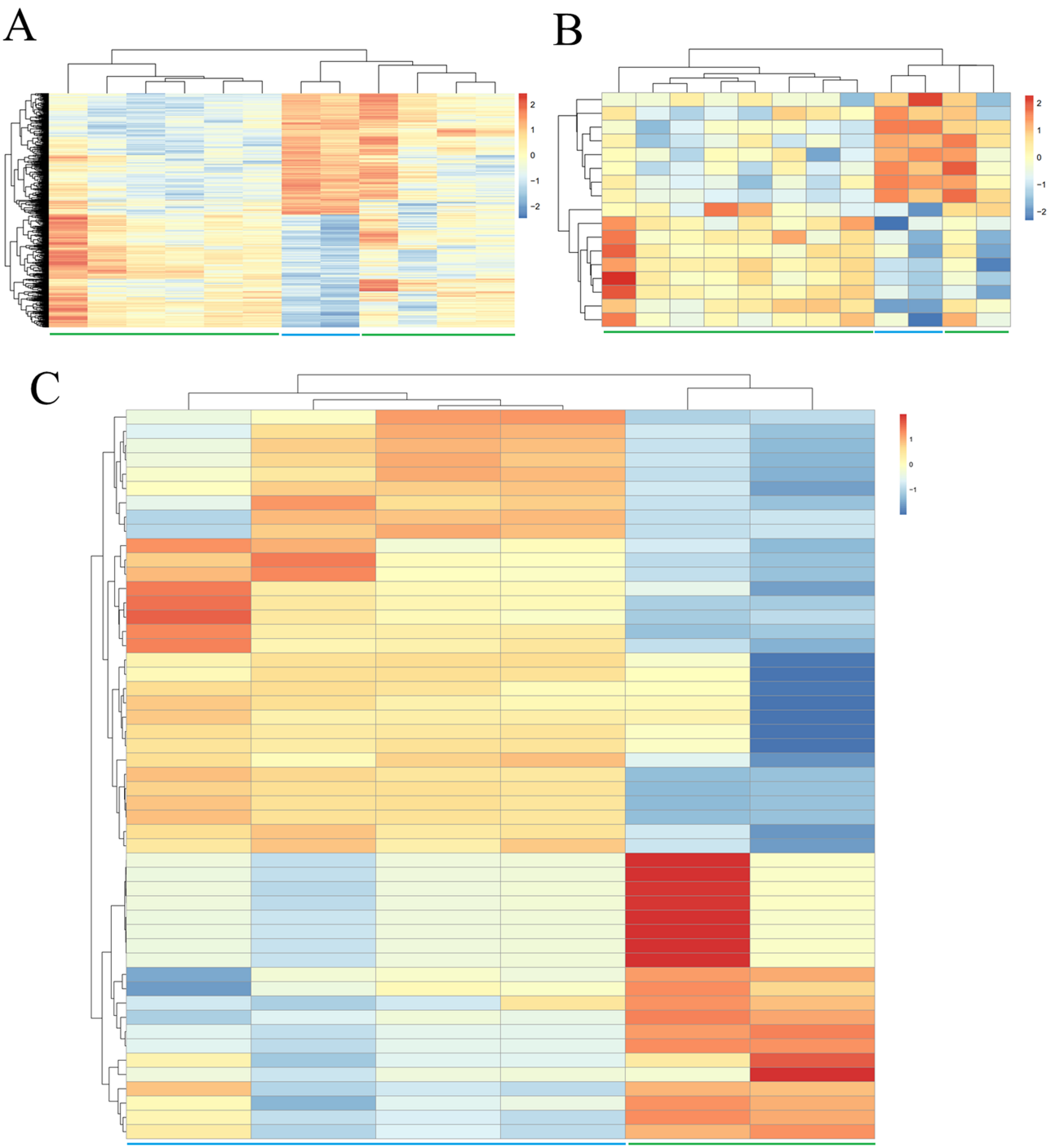

Figure 1 Hierarchical clustering and heat map analysis of differentially expressed (A) genes, (B) long non-coding RNAs and (C) microRNAs. Red, high expression; light blue, low expression. Full-size DOI: 10.7717/peerj.7544/fig-1

differentially expressed transcription factor to regulate the other target genes in the PPI network using IRegulon plug-in (Fig. 4), indicating FOXO1 was also a hub gene.

Function analysis showed eight significant KEGG pathways were enriched, including hsa04015:Rap1 signaling pathway (PIK3R1), hsa05200:Pathways in cancer (PIK3R1,

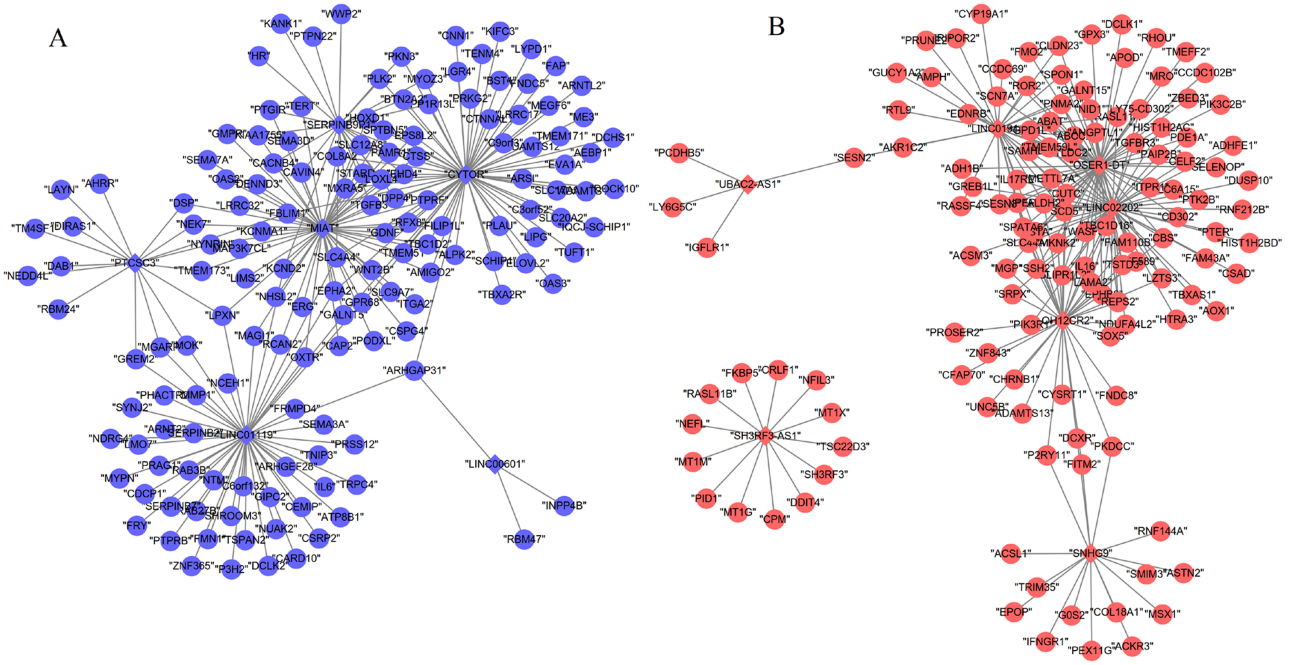

Figure 2 Co-expression network between differentially expressed long non-coding RNAs and genes. (A) Downregulated lncRNA–mRNA co-expression (blue); (B) upregulated lncRNA–mRNA co-expression (red). Circular, differentially expressed genes; rhombus, differentially expressed long non-coding RNAs.
Full-size DOI: 10.7717/peerj.7544/fig-2

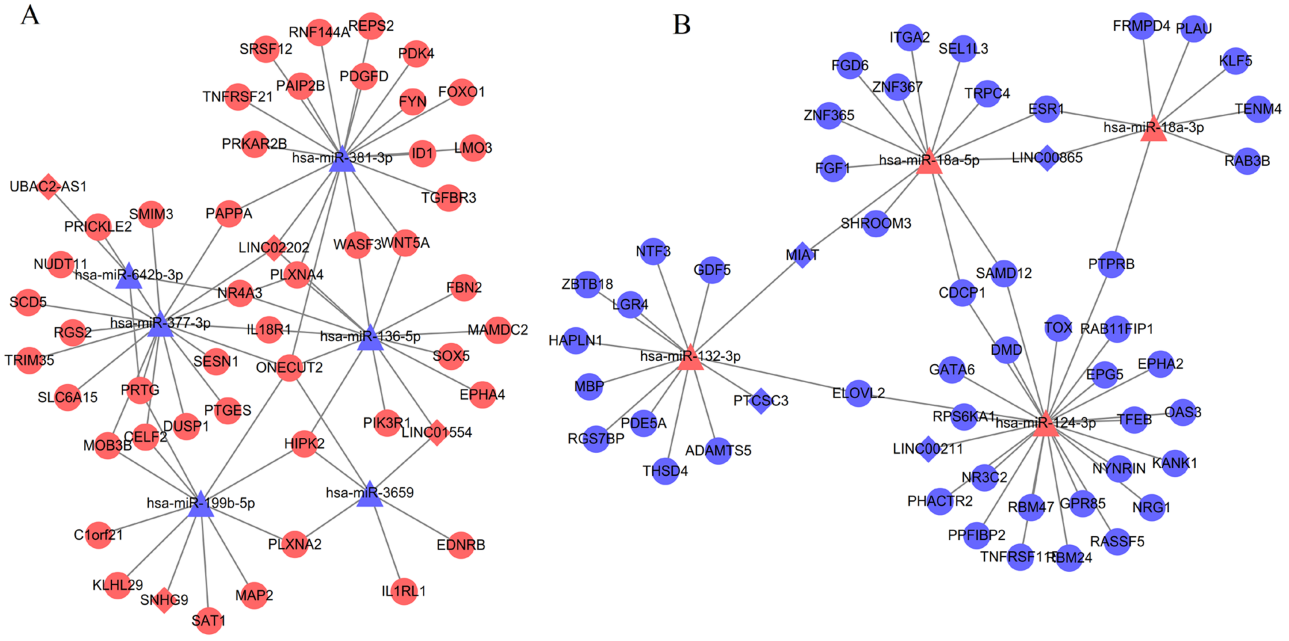

Figure 3 Competing endogenous RNA network (ceRNA) among differentially expressed long non-coding RNAs, microRNAs and genes. (A) Downregulated ceRNA axes according to the expression of miRNAs; (B) upregulated ceRNA axes according to the expression of miRNAs. Red, upregulated; blue, downregulated. Circular, differentially expressed genes; rhombus, differentially expressed long non-coding RNAs; triangle, microRNAs.
Full-size DOI: 10.7717/peerj.7544/fig-3

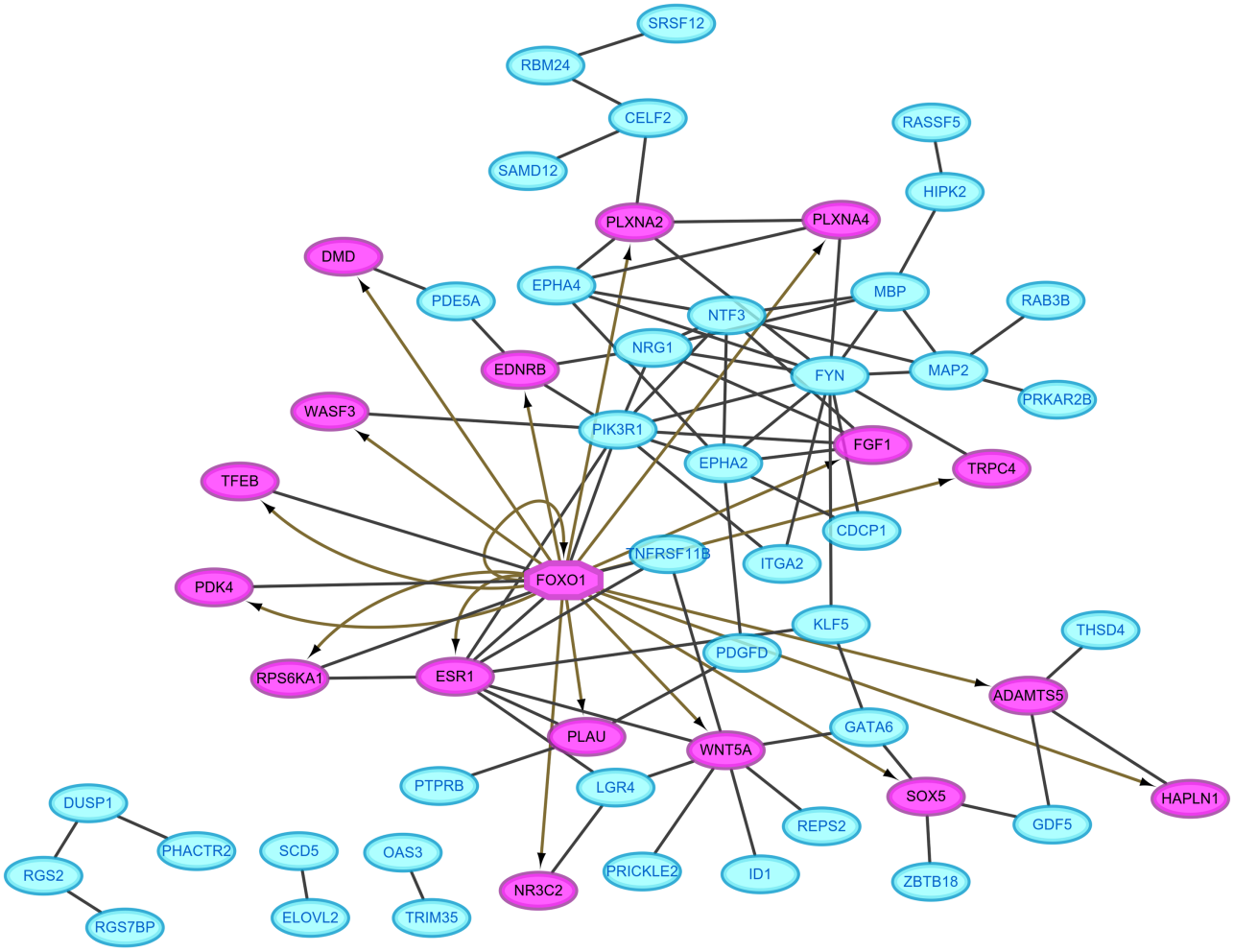

Figure 4 Protein–protein interaction network. Red, upregulated; blue, downregulated. Oval, differentially expressed genes; hexagon, differentially expressed transcription factor. Full-size DOI: 10.7717/peerj.7544/fig-4

Table 2 Hub genes in the protein-protein network screened by topological features.

Gene	Degree		Betweenness		Closeness		Eigenvector
FYN	12	FYN	983.10	FYN	0.096	FYN	0.42
PIK3R1	10	PIK3R1	716.77	PIK3R1	0.096	PIK3R1	0.39
ESR1	8	ESR1	658.76	KLF5	0.095	NTF3	0.33
NTF3	7	GATA6	543.73	ESR1	0.095	EPHA2	0.32
EPHA2	7	KLF5	529.64	EPHA2	0.093	NRG1	0.30
WNT5A	7	SOX5	438	NRG1	0.093	EPHA4	0.24
NRG1	6	WNT5A	405.05	FOXO1	0.092	FGF1	0.24
FOXO1	6	PLXNA2	352	NTF3	0.092	MBP	0.22
EPHA4	5	CELF2	274	ITGA2	0.092	MAP2	0.18
MBP	5	GDF5	270	GATA6	0.091	ESR1	0.15

Table 3 KEGG pathway enrichment for the genes in the PPI network.

Term	*p*-Value	Genes
hsa04015:Rap1 signaling pathway	2.25*E*-03	RASSF5, ID1, PDGFD, FGF1, PIK3R1, EPHA2
hsa05200:Pathways in cancer	7.28*E*-03	WNT5A, EDNRB, RASSF5, FOXO1, ITGA2, FGF1, PIK3R1
hsa05205:Proteoglycans in cancer	1.18*E*-02	WNT5A, ESR1, ITGA2, PIK3R1, PLAU
hsa04014:Ras signaling pathway	1.78*E*-02	RASSF5, PDGFD, FGF1, PIK3R1, EPHA2
hsa04360:Axon guidance	1.90*E*-02	EPHA4, FYN, PLXNA2, EPHA2
hsa04390:Hippo signaling pathway	2.97*E*-02	WNT5A, ID1, GDF5, FGF1
hsa04520:Adherens junction	4.03*E*-02	PTPRB, WASF3, FYN
hsa05218:Melanoma	4.03*E*-02	PDGFD, FGF1, PIK3R1

FOXO1), hsa05205:Proteoglycans in cancer (ESR1, PIK3R1), hsa04014:Ras signaling pathway (PIK3R1), hsa05218:Melanoma (PIK3R1) and hsa04520:Adherens junction (PTPRB) (Table 3).

In addition, 79 GO biological process terms were also enriched, such as GO:0042981—regulation of apoptotic process (ESR1), GO:0045893—positive regulation of transcription, DNA-templated (ESR1, FOXO1), GO:0043066—negative regulation of apoptotic process (FOXO1, PIK3R1), GO:0014066—regulation of phosphatidylinositol 3-kinase signaling (PIK3R1), GO:0048146—positive regulation of fibroblast proliferation (ESR1), GO:0001525—angiogenesis (PTPRB) and GO:0001678—cellular glucose homeostasis (FOXO1, PIK3R1) (Table 4; Supplemental Information 5).

Integrated analysis to identify crucial lncRNAs

By comparing the co-expression with ceRNA networks, five lncRNAs (SNHG9, LINC02202, UBAC2-AS1, PTCSC3 and myocardial infarction associated transcript (MIAT)) and 32 genes (such as PIK3R1, PTPRB) were found to be shared.

By comparing the hub genes enriched into KEGG pathways with the genes regulated by the above five lncRNAs (SNHG9, LINC02202, UBAC2-AS1, PTCSC3 and MIAT), we found the following ceRNA and co-expression axes may be important, including LINC02202 (upregulated)-hsa-miR-136-5p (downregulated)-PIK3R1 (upregulated), LINC02202 (upregulated)-hsa-miR-381-3p (downregulated)-FOXO1 (upregulated), MIAT (downregulated)-hsa-miR-18a-5p (upregulated)-ESR1 (downregulated) and LINC02202 (downregulated)-PIK3R1(downregulated). Furthermore, the comparison between hub genes enriched into KEGG pathways and the shared genes in two networks also indicated PTPRB related co-expression axis (LINC01119 (downregulated)-PTPRB (downregulated)) was also crucial.

DISCUSSION

In present study, we identified three crucial lncRNAs (MIAT, LINC02202 and LINC01119) for adipogenesis from human ASCs. MIAT may sponge hsa-miR-18a-5p and influence the inhibition of hsa-miR-18a-5p on the expression of ESR1. LINC02202 may function as a ceRNA for hsa-miR-136-5p/hsa-miR-381-3p to respectively regulate the expressions

Table 4 GO biological process term enrichment for the genes in the PPI network.

Term	*p*-Value	Genes
GO:0042981—regulation of apoptotic process	6.04*E*-05	RASSF5, TNFRSF11B, DUSP1, NTF3, FYN, GDF5, ESR1
GO:0032148—activation of protein kinase B activity	7.76*E*-05	WNT5A, NTF3, FGF1, NRG1
GO:0007596—blood coagulation	3.06*E*-04	PRKAR2B, FYN, GATA6, ITGA2, PDGFD, PLAU
GO:0071560—cellular response to transforming growth factor beta stimulus	5.22*E*-04	WNT5A, FYN, SOX5, PDGFD
GO:0043066—negative regulation of apoptotic process	6.03*E*-04	WNT5A, EDNRB, DUSP1, RPS6KA1, ID1, GATA6, FOXO1, PIK3R1
GO:0045944—positive regulation of transcription from RNA polymerase II promoter	1.01*E*-03	KLF5, WNT5A, RPS6KA1, GATA6, HIPK2, TFEB, ESR1, FOXO1, FGF1, NRG1, PIK3R1
GO:0045893—positive regulation of transcription, DNA-templated	1.25*E*-03	KLF5, WNT5A, GATA6, HIPK2, TFEB, ESR1, FOXO1, LGR4
GO:0018108—peptidyl-tyrosine phosphorylation	1.47*E*-03	EPHA4, FYN, FGF1, NRG1, EPHA2
GO:0014066—regulation of phosphatidylinositol 3-kinase signaling	2.02*E*-03	FYN, FGF1, NRG1, PIK3R1
GO:0030335—positive regulation of cell migration	2.88*E*-03	NTF3, PDGFD, FGF1, PIK3R1, PLAU
GO:0046854—phosphatidylinositol phosphorylation	3.43*E*-03	FYN, FGF1, NRG1, PIK3R1
GO:0030182—neuron differentiation	3.53*E*-03	WNT5A, ID1, HIPK2, EPHA2
GO:0008284—positive regulation of cell proliferation	3.70*E*-03	KLF5, EDNRB, NTF3, HIPK2, PDGFD, FGF1, NRG1
GO:0048015—phosphatidylinositol-mediated signaling	4.80*E*-03	FYN, FGF1, NRG1, PIK3R1
GO:0000187—activation of MAPK activity	4.93*E*-03	WNT5A, NTF3, FGF1, NRG1
GO:0045892—negative regulation of transcription, DNA-templated	5.16*E*-03	WNT5A, ID1, GATA6, FOXO1, NRG1, ZBTB18, LGR4
GO:0045766—positive regulation of angiogenesis	6.02*E*-03	WNT5A, GATA6, HIPK2, FGF1
GO:0000122—negative regulation of transcription from RNA polymerase II promoter	7.94*E*-03	KLF5, EDNRB, ID1, GATA6, HIPK2, ESR1, FOXO1, ZBTB18
GO:0043524—negative regulation of neuron apoptotic process	8.79*E*-03	NTF3, FYN, GDF5, HIPK2
GO:0035556—intracellular signal transduction	9.37*E*-03	PRKAR2B, RASSF5, DUSP1, RPS6KA1, FYN, NRG1
GO:0045213—neurotransmitter receptor metabolic process	9.62*E*-03	DMD, NRG1
GO:0060750—epithelial cell proliferation involved in mammary gland duct elongation	1.28*E*-02	WNT5A, ESR1
GO:0048146—positive regulation of fibroblast proliferation	1.31*E*-02	WNT5A, ESR1, PDGFD
GO:0043406—positive regulation of MAP kinase activity	1.54*E*-02	PDE5A, PDGFD, FGF1
GO:0043627—response to estrogen	1.86*E*-02	TNFRSF11B, GATA6, ESR1
GO:0014068—positive regulation of phosphatidylinositol 3-kinase signaling	1.86*E*-02	FYN, PDGFD, NRG1
GO:0048841—regulation of axon extension involved in axon guidance	2.23*E*-02	PLXNA4, PLXNA2
GO:0008366—axon ensheathment	2.23*E*-02	NRG1, MBP
GO:0050966—detection of mechanical stimulus involved in sensory perception of pain	2.54*E*-02	FYN, ITGA2
GO:0008286—insulin receptor signaling pathway	2.61*E*-02	PDK4, FOXO1, PIK3R1
GO:0090630—activation of GTPase activity	2.67*E*-02	WNT5A, NTF3, EPHA2

(Continued)

Table 4 (continued).

Term	*p*-Value	Genes
GO:0060068—vagina development	2.89*E*-02	WNT5A, ESR1
GO:0021785—branchiomotor neuron axon guidance	2.86*E*-02	PLXNA4, PLXNA2
GO:0007165—signal transduction	3.11*E*-02	TNFRSF11B, NTF3, RPS6KA1, PDE5A, NR3C2, ESR1, FGF1, PIK3R1, PLAU
GO:0048013—ephrin receptor signaling pathway	3.12*E*-02	EPHA4, FYN, EPHA2
GO:0031643—positive regulation of myelination	3.17*E*-02	WASF3, NRG1
GO:0010976—positive regulation of neuron projection development	3.33*E*-02	WNT5A, FYN, DMD
GO:1901653—cellular response to peptide	3.48*E*-02	KLF5, ID1
GO:0046849—bone remodeling	3.48*E*-02	LGR4, EPHA2
GO:0033628—regulation of cell adhesion mediated by integrin	3.48*E*-02	EPHA2, PLAU
GO:0001525—angiogenesis	3.49*E*-02	KLF5, PTPRB, ID1, FGF1
GO:0007179—transforming growth factor beta receptor signaling pathway	3.53*E*-02	ID1, GDF5, HIPK2
GO:0008584—male gonad development	3.68*E*-02	WNT5A, GATA6, ESR1
GO:1902287—semaphorin-plexin signaling pathway involved in axon guidance	3.79*E*-02	PLXNA4, PLXNA2
GO:0055119—relaxation of cardiac muscle	3.79*E*-02	RGS2, PDE5A
GO:0007169—transmembrane receptor protein tyrosine kinase signaling pathway	3.82*E*-02	NTF3, FYN, NRG1
GO:0001678—cellular glucose homeostasis	4.41*E*-02	FOXO1, PIK3R1
GO:0060065—uterus development	4.41*E*-02	WNT5A, ESR1
GO:0006636—unsaturated fatty acid biosynthetic process	4.72*E*-02	ELOVL2, SCD5

of PIK3R1 and FOXO1; LINC02202 also may directly affect the transcription of PIK3R1. LINC01119 may co-express with PTPRB to impact its transcription. Although all these relationship pairs may be potentially important, LINC01119–PTPRB co-expression axis may be especially verifiable because their expression significance met the criterion of adjusted p-value < 0.05.

Although there have studies to show the roles of lncRNA MIAT for stem differentiation, only osteogenic (*Jin et al., 2017*) and endothelial cell (*Wang et al., 2018*) differentiation were investigated, without evidence to prove its effect on adipogenesis of human ASCs. A recent study revealed MIAT was an estrogen-inducible lncRNA and its expression was positively related to estrogen receptor (*Li et al., 2018b*). There was accumulating evidence to reveal that exposure of bone marrow stem cells to icariin or flavonoids of Herba Epimedii inhibited adipogenic differentiation, exhibiting decreased adipocyte numbers and downregulated mRNA expression of adipogenic differentiation markers, peroxisome proliferator-activated receptor gamma (PPARγ) and CCAAT/enhancer-binding protein α (C/EBPα) (*Li et al., 2018c*; *Zhang et al., 2015*); while treatment of bone marrow stem cells with estrogen receptor antagonist ICI182780 revered the effects of Herba Epimedii ingredient and promoted adipogenesis (*Li et al., 2018c*; *Zhang et al., 2015*). The study of

Ihunnah et al. (2014) also demonstrated activation of estrogen receptor in ASCs inhibited adipogenesis by decreasing the recruitment of the adipogenic PPARγ onto its target gene promoters, whereas the use of estrogen receptor antagonism ICI 182780 or knockdown of estrogen receptor-α via lentiviral shRNA enhanced adipogenesis by increasing the expression of PPARγ. Thus, it can be hypothesized that MIAT may be lower expressed in adipogenic differentiation cells like ESR1, which was also confirmed in our study. However, the interaction mechanisms between MIAT and estrogen receptor remain unclear. In present study, we predicted that downregulated MIAT may be insufficient to sponge hsa-miR-18a-5p and lead to more hsa-miR-18a-5p to bind with the 3′ untranslated region of ESR1, inducing the lower expression of ESR1. This hypothesis may be indirectly demonstrated by the fact that miR-18a mimic significantly promoted mesenchymal stem cell (MSC) adipogenic differentiation, while the addition of miR-18a inhibitor obtained the negative effects on adipogenic differentiation of MSCs (*Li et al., 2018a*). The negative regulatory relationship between ESR1 and miR-18a were also validated in human trophoblast cell line by the luciferase assay (*Zhu et al., 2015*).

LINC02202 may be a newly identified lncRNA associated with stem cell differentiation because its role had not been previously mentioned in the literatures. In this study, we predicted upregulated LINC02202 may be involved in ASCs adipogenic differentiation by regulating phosphatidylinositol 3-kinase (PI3K) signaling. It has been reported that PI3K signaling pathway was strongly activated in MSCs under the adipogenesis-inducing hormone cocktail (*Kim et al., 2017*), and the addition of PI3K specific inhibitor LY294002 severely suppressed lipid accumulation, as well as the expression of adipogenic markers PPARγ and C/EBPα (*Yu et al., 2008*). PIK3R1 is a critical component of the PI3K signaling pathway and its expression was also demonstrated to be increased after the induction of adipocyte differentiation from preadipocytes 3T3-L1 (*Kim et al., 2014a*). Thus, theoretically, PIK3R1 may be upregulated in adipogenic differentiation cells compared with undifferentiated human ASCs, which was confirmed in our study. Activated PI3K/AKT signaling may promote adipogenesis through upregulating downstream transcription factors, such as FoxO1 (*Yi et al., 2018*) which may subsequently enhance the transcription of its target genes, PPAR-γ and C/EBP-α (*Ambele et al., 2016*; *Munekata & Sakamoto, 2009*); whereas persistent inhibition of FoxO1 with its antagonist AS1842856 (*Zou et al., 2014*) or knockdown of FoxO1 (*Sun et al., 2017*) was also observed to almost completely suppress adipocyte differentiation and lipogenesis. As expected, we also found FoxO1 was significantly high expressed during adipogenic differentiation. In addition to directly affect the transcription of PIK3R1, LINC02202 may function as a ceRNA for miR-136-5p and hsa-miR-381-3p to regulate the expression of PIK3R1a and FoxO1, respectively. Although there was no study to demonstrate these ceRNA interaction axes, the negative correlation between the expression of miR-136 and adipogenic markers C/EBPα and PPARα in subcutaneous adipose tissue of lambs may indirectly illuminate the importance of miR-136 for adipogenic differentiation (*Meale et al., 2014*). As expected, we also found miR-136-5p was significantly downregulated in adipogenic differentiation cells.

There was only one sequencing study to identify that LINC01119 was downregulated in colorectal cancer cells after hypoxia treatment (*Han et al., 2019*). Several authors had

demonstrated hypoxia exposure was effective to enhance adipocyte differentiation from ASCs (*Fink et al., 2004*; *Valorani et al., 2012*; *Kim et al., 2014b*), which was medicated by the generation of reactive oxygen species (ROS) and activation of PI3K/Akt/mTOR (*Kim et al., 2014b*); the addition of ROS scavenger or Akt/mTOR inhibitor prevented adipocyte differentiation (*Kim et al., 2014b*). Thus, LINC01119 may have anti-adipose differentiation potential and lower expressed in adipogenic differentiation cells compared with undifferentiated human ASCs, which was validated in our study. However, its mechanisms for adipocyte differentiation remain unclear. We predicted LINC01119 may co-express with PTPRB. The study of Kim et al. showed ectopic over-expression of PTPRB inhibited the expression of adipocyte-related genes (such as PPAR-γ) and led to a reduced adipocyte differentiation from preadipocytes. Also, PTPRB was reported to suppress the tyrosine phosphorylation of VEGFR2 during adipocyte differentiation (*Kim et al., 2019*). Generally, VEGF functions by binding with VEGFR2, while transfection of VEGF to ASCs increased fat cell survival (*Zhang et al., 2017*). These findings suggest PTPRB may also be downregulated to promote VEGF secretion and activate its mediated pathways, ultimately inducing adipogenic differentiation from ASCs. This hypothesis was in line with our study showing PTPRB was lower expressed in adipocyte differentiation cells and was involved in angiogenesis.

There are some limitations in this study. First, only two datasets were submitted between 5 years until now, and not all were used for this analysis, which may cause some bias in results due to the small sample size and different data platforms. However, we believe the sequencing or microarray technology may be more mature recently and thus the results may be more believable. This was also indirectly reflected by the less overlapped genes if the other datasets were used (only two comparing GSE72429 with GSE25715; *Guo & Cao, 2019*) and thus, we renounced the use of multiple datasets and only the newly one. Moreover, this work investigated lncRNA co-expression and ceRNA mechanisms, which required the lncRNA and mRNA should be simultaneously analyzed. Thus, some datasets that only independently investigated lncRNA or mRNA were also excluded. Second, the crucial co-expression and ceRNA axes were obtained by database prediction, which may lead to many false positives. Therefore, further in vitro wet experiments (PCR, luciferase assay, knockdown or overexpression) are still indispensable to confirm the interaction between lncRNAs and miRNAs, lncRNA and mRNAs as well as the miRNAs and mRNAs and their roles during adipogenic differentiation of ASCs.

CONCLUSION

The present study preliminarily identified three new targets (lncRNA MIAT, LINC02202 and LINC01119) for inducing adipogenesis from human ASCs and promoting facial soft tissue reconstruction. They may be involved in adipogenesis by acting as a ceRNA (LINC02202-miR-136-5p-PIK3R1, LINC02202-miR-381-3p-FOXO1 and MIAT-miR-18a-5p-ESR1) or co-expressing with its targets (LINC02202-PIK3R1, LINC01119-PTPRB).

ADDITIONAL INFORMATION AND DECLARATIONS

Funding

The authors received no funding for this work.

Competing Interests

The authors declare that they have no competing interests.

Author Contributions

- Kana Chen conceived and designed the experiments, performed the experiments, analyzed the data, contributed reagents/materials/analysis tools, prepared figures and/or tables, authored or reviewed drafts of the paper, approved the final draft.
- Shujie Xie analyzed the data, prepared figures and/or tables, approved the final draft.
- Wujun Jin conceived and designed the experiments, authored or reviewed drafts of the paper, approved the final draft.

Data Availability

The following information was supplied regarding data availability:

Raw data is available in Supplemental Files.

Supplemental Information

Supplemental information for this article can be found online at http://dx.doi.org/10.7717/peerj.7544#supplemental-information.

REFERENCES

Ambele MA, Dessels C, Durandt C, Pepper MS. 2016. Genome-wide analysis of gene expression during adipogenesis in human adipose-derived stromal cells reveals novel patterns of gene expression during adipocyte differentiation. *Stem Cell Research* **16(3)**:725–734 DOI 10.1016/j.scr.2016.04.011.

Bashir MM, Sohail M, Bashir A, Khan FA, Jan SN, Imran M, Ahmad FJ, Choudhery MS. 2018. Outcome of conventional adipose tissue grafting for contour deformities of face and role of ex vivo expanded adipose tissue-derived stem cells in treatment of such deformities. *Journal of Craniofacial Surgery* **29**:1143–1147 DOI 10.1097/SCS.0000000000004367.

Charles-De-Sá L, Gontijo-De-Amorim NF, Maeda Takiya C, Borojevic R, Benati D, Bernardi P, Sbarbati A, Rigotti G. 2015. Antiaging treatment of the facial skin by fat graft and adipose-derived stem cells. *Plastic and Reconstructive Surgery* **135(4)**:999–1009 DOI 10.1097/PRS.0000000000001123.

Dweep H, Gretz N. 2015a. miRWalk2.0. Heidelberg: Heidelberg University. *Available at http://zmf.umm.uni-heidelberg.de/apps/zmf/mirwalk2/index.html*.

Dweep H, Gretz N. 2015b. miRWalk2.0: a comprehensive atlas of microRNA-target interactions. *Nature Methods* **12(8)**:697–697 DOI 10.1038/nmeth.3485.

Fink T, Abildtrup L, Fogd K, Abdallah BM, Kassem M, Ebbesen P, Zachar V. 2004. Induction of adipocyte-like phenotype in human mesenchymal stem cells by hypoxia. *Stem Cells* **22(7)**:1346–1355 DOI 10.1634/stemcells.2004-0038.

Guo Z, Cao Y. 2019. An lncRNA-miRNA-mRNA ceRNA network for adipocyte differentiation from human adipose-derived stem cells. *Molecular Medicine Reports* **19**:4271–4287 DOI 10.3892/mmr.2019.10067.

Han Y, Wang X, Mao E, Shen B, Huang L. 2019. Analysis of differentially expressed lncRNAs and mRNAs for the identification of hypoxia-regulated angiogenic genes in colorectal cancer by RNA-seq. *Medical Science Monitor* **25**:2009–2015 DOI 10.12659/MSM.915179.

Huang Y, Jin C, Zheng Y, Li X, Zhang S, Zhang Y, Jia L, Li W. 2017. Knockdown of lncRNA MIR31HG inhibits adipocyte differentiation of human adipose-derived stem cells via histone modification of FABP4. *Scientific Reports* **7(1)**:8080 DOI 10.1038/s41598-017-08131-6.

Huang DW, Sherman BT, Lempicki RA. 2009. Systematic and integrative analysis of large gene lists using DAVID bioinformatics resources. *Nature Protocols* **4(1)**:44–57 DOI 10.1038/nprot.2008.211.

Huang M, Zhong Z, Lv M, Shu J, Tian Q, Chen J. 2016. Comprehensive analysis of differentially expressed profiles of lncRNAs and circRNAs with associated co-expression and ceRNA networks in bladder carcinoma. *Oncotarget* **7**:47186–47200 DOI 10.18632/oncotarget.9706.

Ihunnah CA, Wada T, Philips BJ, Ravuri SK, Gibbs RB, Kirisci L, Rubin JP, Marra KG, Xie W. 2014. Estrogen sulfotransferase/SULT1E1 promotes human adipogenesis. *Molecular and Cellular Biology* **34(9)**:1682–1694 DOI 10.1128/MCB.01147-13.

Janky R, Verfaillie A, Imrichová H, Van De Sande B, Standaert L, Christiaens V, Hulselmans G, Herten K, Naval Sanchez M, Potier D, Svetlichnyy D, Kalender Atak Z, Fiers M, Marine JC, Aerts S. 2014. iRegulon: from a gene list to a gene regulatory network using large motif and track collections. *PLOS Computational Biology* **10(7)**:e1003731 DOI 10.1371/journal.pcbi.1003731.

Jeggari A, Marks DS, Larsson E. 2012. miRcode: a map of putative microRNA target sites in the long non-coding transcriptome. *Bioinformatics* **28(15)**:2062–2063 DOI 10.1093/bioinformatics/bts344.

Jin C, Zheng Y, Huang Y, Liu Y, Jia L, Zhou Y. 2017. Long non-coding RNA MIAT knockdown promotes osteogenic differentiation of human adipose-derived stem cells. *Cell Biology International* **41(1)**:33–41 DOI 10.1002/cbin.10697.

Kim J, Han D, Byun SH, Kwon M, Cho SJ, Koh YH, Yoon K. 2017. Neprilysin facilitates adipogenesis through potentiation of the phosphatidylinositol 3-kinase (PI3K) signaling pathway. *Molecular and Cellular Biochemistry* **430(1–2)**:1–9 DOI 10.1007/s11010-017-2948-6.

Kim YJ, Kim HJ, Chung KY, Choi I, Kim SH. 2014a. Transcriptional activation of PIK3R1 by PPARγ in adipocytes. *Molecular Biology Reports* **41(8)**:5267–5272 DOI 10.1007/s11033-014-3398-9.

Kim JS, Kim WK, Oh KJ, Lee EW, Han BS, Lee SC, Bae KH. 2019. Protein tyrosine phosphatase, receptor type B (PTPRB) inhibits brown adipocyte differentiation through regulation of VEGFR2 phosphorylation. *Journal of Microbiology and Biotechnology* **29(4)**:645–650 DOI 10.4014/jmb.1810.10033.

Kim JH, Kim SH, Song SY, Kim WS, Song SU, Yi TG, Jeon MS, Chung HM, Xia Y, Sung JH. 2014b. Hypoxia induces adipocyte differentiation of adipose-derived stem cells by triggering reactive oxygen species generation. *Cell Biology International* **38(1)**:32–40 DOI 10.1002/cbin.10170.

Kohl M, Wiese S, Warscheid B. 2011. Cytoscape: software for visualization and analysis of biological networks. *Methods in Molecular Biology* **696**:291–303 DOI 10.1007/978-1-60761-987-1_18.

Kolde R. 2019. pheatmap: pretty heatmaps. Vienna: the R foundation for statistical computing. *Available at https://cran.r-project.org/package=pheatmap*.

Kotaro Y, Katsujiro S, Noriyuki A, Masakazu K, Keita I, Hirotaka S, Hitomi E, Harunosuke K, Toshitsugu H, Kiyonori H. 2008. Cell-assisted lipotransfer for facial lipoatrophy: efficacy of clinical use of adipose-derived stem cells. *Dermatologic Surgery* **34**:1178–1185 DOI 10.1111/j.1524-4725.2008.34256.x.

Langfelder P, Horvath S. 2016. Tutorials for the WGCNA package. *Available at https://horvath.genetics.ucla.edu/html/CoexpressionNetwork/Rpackages/WGCNA/Tutorials/*.

Li X, Ao J, Wu J. 2017. Systematic identification and comparison of expressed profiles of lncRNAs and circRNAs with associated co-expression and ceRNA networks in mouse germline stem cells. *Oncotarget* **8**:26573–26590 DOI 10.18632/oncotarget.15719.

Li Y, Jiang B, Wu X, Huang Q, Chen W, Zhu H, Qu X, Xie L, Ma X, Huang G. 2018b. Long non-coding RNA MIAT is estrogen-responsive and promotes estrogen-induced proliferation in ER-positive breast cancer cells. *Biochemical and Biophysical Research Communications* **503(1)**:45–50 DOI 10.1016/j.bbrc.2018.05.146.

Li Z, Jin C, Chen S, Zheng Y, Huang Y, Jia L, Ge W, Zhou Y. 2017. Long non-coding RNA MEG3 inhibits adipogenesis and promotes osteogenesis of human adipose-derived mesenchymal stem cells via miR-140-5p. *Molecular and Cellular Biochemistry* **433(1–2)**:51–60 DOI 10.1007/s11010-017-3015-z.

Li JH, Liu S, Zhou H, Qu LH, Yang JH. 2014. starBase v2.0: decoding miRNA-ceRNA, miRNA-ncRNA and protein-RNA interaction networks from large-scale CLIP-Seq data. *Nucleic Acids Research* **42(D1)**:D92–D97 DOI 10.1093/nar/gkt1248.

Li X, Peng B, Pan Y, Wang P, Sun K, Lei X, Ou L, Wu Z, Liu X, Wang H, He H, Mo S, Tian Y, Peng X, Zhu X, Zhang R, Yang L. 2018c. Icariin stimulates osteogenic differentiation and suppresses adipogenic differentiation of rBMSCs via estrogen receptor signaling. *Molecular Medicine Reports* **18**:3483–3489 DOI 10.3892/mmr.2018.9325.

Li M, Xie Z, Wang P, Li J, Liu W, Tang SA, Liu Z, Wu X, Wu Y, Shen H. 2018a. The long noncoding RNA GAS5 negatively regulates the adipogenic differentiation of MSCs by modulating the miR-18a/CTGF axis as a ceRNA. *Cell Death & Disease* **9(5)**:554 DOI 10.1038/s41419-018-0627-5.

Ma L, Wen H, Jian X, Liao H, Sui Y, Liu Y, Xu G. 2015. Cell-assisted lipotransfer in the clinical treatment of facial soft tissue deformity. *Plastic Surgery* **23(3)**:199–202 DOI 10.1177/229255031502300304.

Meale SJ, Romao JM, He ML, Chaves AV, McAllister TA, Guan LL. 2014. Effect of diet on microRNA expression in ovine subcutaneous and visceral adipose tissues. *Journal of Animal Science* **92(8)**:3328–3337 DOI 10.2527/jas.2014-7710.

Munekata K, Sakamoto K. 2009. Forkhead transcription factor Foxo1 is essential for adipocyte differentiation. *In Vitro Cellular & Developmental Biology–Animal* **45**:642–651 DOI 10.1007/s11626-009-9230-5.

Nuermaimaiti N, Liu J, Liang X, Jiao Y, Zhang D, Liu L, Meng X, Guan Y. 2018. Effect of lncRNA HOXA11-AS1 on adipocyte differentiation in human adipose-derived stem cells. *Biochemical and Biophysical Research Communications* **495(2)**:1878–1884 DOI 10.1016/j.bbrc.2017.12.006.

Paraskevopoulou MD, Georgakilas G, Kostoulas N, Reczko M, Maragkakis M, Dalamagas TM, Hatzigeorgiou AG. 2013. DIANA-LncBase: experimentally verified and computationally predicted microRNA targets on long non-coding RNAs. *Nucleic Acids Research* **41(D1)**:D239–D245 DOI 10.1093/nar/gks1246.

Paraskevopoulou MD, Vlachos IS, Karagkouni D, Georgakilas G, Kanellos I, Vergoulis T, Zagganas K, Tsanakas P, Floros E, Dalamagas T, Hatzigeorgiou AG. 2019. LncBase Predicted v.2. Volos: University of Thessaly. *Available at http://carolina.imis.athena-innovation.gr/diana_tools/web/index.php?r=lncbasev2/index-predicted*.

Philips BJ, Marra KG, Rubin JP. 2014. Healing of grafted adipose tissue: current clinical applications of adipose-derived stem cells for breast and face reconstruction. *Wound Repair and Regeneration* **22(Suppl)**:11–13 DOI 10.1111/wrr.12164.

Rauch A, Haakonsson AK, Madsen JGS, Larsen M, Forss I, Madsen MR, Van Hauwaert EL, Wiwie C, Jespersen NZ, Tencerova M, Nielsen R, Larsen BD, Röttger R, Baumbach J, Scheele C, Kassem M, Mandrup S. 2019. Osteogenesis depends on commissioning of a network of stem cell transcription factors that act as repressors of adipogenesis. *Nature Genetics* **51(4)**:716–727 DOI 10.1038/s41588-019-0359-1.

Ritchie ME, Phipson B, Wu D, Hu Y, Law CW, Shi W, Smyth GK. 2015. Limma. Seattle: Bioconductor. *Available at https://bioconductor.org/packages/release/bioc/html/limma.html*.

Shannon P, Markiel A, Ozier O, Baliga NS, Wang JT, Ramage D, Amin N, Schwikowski B, Ideker T. 2001–2008. Cytoscape. *Available at https://cytoscape.org/*.

Sun YM, Qin J, Liu SG, Cai R, Chen XC, Wang XM, Pang WJ. 2017. PDGFRα regulated by miR-34a and FoxO1 promotes adipogenesis in porcine intramuscular preadipocytes through Erk signaling pathway. *International Journal of Molecular Sciences* **18(11)**:2424 DOI 10.3390/ijms18112424.

Szklarczyk D, Franceschini A, Wyder S, Forslund K, Heller D, Huerta-Cepas J, Simonovic M, Roth A, Santos A, Tsafou KP, Kuhn M, Bork P, Jensen LJ, Von Mering C. 2015. STRING v10: protein-protein interaction networks, integrated over the tree of life. *Nucleic Acids Research* **43(D1)**:D447–D452 DOI 10.1093/nar/gku1003.

Szklarczyk D, Gable AL, Lyon D, Junge A, Wyder S, Huerta-Cepas J, Simonovic M, Doncheva NT, Morris JH, Bork P, Jensen LJ, von Mering C. 2019. STRING. Lausanne: Swiss Institute of Bioinformatics. *Available at https://string-db.org/*.

Tang Y, Li M, Wang J. 2014. CytoNCA. San Diego: Cytoscape. *Available at http://apps.cytoscape.org/apps/cytonca*.

Tang Y, Li M, Wang J, Pan Y, Wu FX. 2015. CytoNCA: a cytoscape plugin for centrality analysis and evaluation of protein interaction networks. *Biosystems* **127**:67–72 DOI 10.1016/j.biosystems.2014.11.005.

Valorani MG, Montelatici E, Germani A, Biddle A, D'Alessandro D, Strollo R, Patrizi MP, Lazzari L, Nye E, Otto WR, Pozzilli P, Alison MR. 2012. Pre-culturing human adipose tissue mesenchymal stem cells under hypoxia increases their adipogenic and osteogenic differentiation potentials. *Cell Proliferation* **45(3)**:225–238 DOI 10.1111/j.1365-2184.2012.00817.x.

Wang H, Ding XG, Yang JJ, Li SW, Zheng H, Gu CH, Jia ZK, Li L. 2018. LncRNA MIAT facilitated BM-MSCs differentiation into endothelial cells and restored erectile dysfunction via targeting miR-200a in a rat model of erectile dysfunction. *European Journal of Cell Biology* **97(3)**:180–189 DOI 10.1016/j.ejcb.2018.02.001.

Yang J. 2010–2013. StarBase v2.0. Guangzhou: Sun Yat-sen University. *Available at http://starbase.sysu.edu.cn/starbase2/*.

Yi L, Chen J, Tao X, Zhou Y, Yuan W, Wang M, Gan Y, Wang K, Xiong S, Cong M. 2018. Epigallocatechin-3-gallate suppresses differentiation of adipocytes via regulating the phosphorylation of FOXO1 mediated by PI3K-AKT signaling in 3T3-L1 cells. *Oncotarget* **9**:7411–7423 DOI 10.18632/oncotarget.23590.

Yu W, Chen Z, Zhang J, Zhang L, Ke H, Huang L, Peng Y, Zhang X, Li S, Lahn BT. 2008. Critical role of phosphoinositide 3-kinase cascade in adipogenesis of human mesenchymal stem cells. *Molecular and Cellular Biochemistry* **310(1–2)**:11–18 DOI 10.1007/s11010-007-9661-9.

Zhang D, Liu L, Jia Z, Yao X, Yang M. 2015. Flavonoids of Herba Epimedii stimulate osteogenic differentiation and suppress adipogenic differentiation of primary mesenchymal stem cells via estrogen receptor pathway. *Pharmaceutical Biology* **54(6)**:954–963 DOI 10.3109/13880209.2015.1079224.

Zhang Y, Xiao LL, Li JX, Liu HW, Li SH, Wu YY, Liao X, Rao CQ. 2017. Improved fat transplantation survival by using the conditioned medium of vascular endothelial growth factor transfected human adipose-derived stem cells. *Kaohsiung Journal of Medical Sciences* **33(8)**:379–384 DOI 10.1016/j.kjms.2017.05.009.

Zhu X, Yang Y, Han T, Yin G, Gao P, Ni Y, Su X, Liu Y, Yao Y. 2015. Suppression of microRNA-18a expression inhibits invasion and promotes apoptosis of human trophoblast cells by targeting the estrogen receptor α gene. *Molecular Medicine Reports* **12(2)**:2701–2706 DOI 10.3892/mmr.2015.3724.

Zou P, Liu L, Zheng L, Liu L, Stoneman RE, Cho A, Emery A, Gilbert ER, Cheng Z. 2014. Targeting FoxO1 with AS1842856 suppresses adipogenesis. *Cell Cycle* **13(23)**:3759–3767 DOI 10.4161/15384101.2014.965977.